Effect of strips size and coating thickness on fluidity of A356 aluminium alloy in lost foam casting process

M. Divandari*, V. Jamali and S. G. Shabestari

In this research, effects of six different strips size (2, 4, 6, 8, 10 and 12 mm thick respectively) and six different coating thicknesses on the fluidity of A356 aluminium alloy in lost foam casting (LFC) process were investigated. It was found that, in each mould, as the strip thickness increases, fluidity length increases. By varying the coating thickness, in a constant strip thickness, the maximum fluidity lengths were obtained in a specific coating thickness. The optimum coating thicknesses to reach maximum fluidity length for 2, 4, 6, 8, 10 and 12 mm strips was measured 170, 250, 250, 280, 350 and 350 μm respectively. This seems to be the result of the simultaneous effects of heat transfer and the controlling roll of permeability of refractory coating. Also the effect of coating thickness on the molten metal velocity in LFC process was studied by using accurate thermal analysis.

Keywords: Coating thickness, Casting thickness, Fluidity, Velocity of molten metal, LFC

Introduction

The A356 aluminium alloy is widely used in aerospace, aircraft and automotive industries due to its high strength to weight ratio, castability, good resistance to corrosion, heat treatability, pressure tightness, etc.[1] For producing lost foam cast components in the mentioned industries, it is important to know the mould filling behaviour of molten metals, especially in thin wall castings and also microstructural characteristics of A356 alloy at various casting thickness. Knowledge of the optimum thickness of coating enables lost foam casting (LFC) manufacturers to ensure that the casting would possibly be produced with less casting defects.[2,3]

In LFC technology, patterns are made by expanded polystyrene (EPS) or expanded polymethyl methacrylate materials.[4] Foam pattern are then coated by a refractory coating slurry, and after drying, they will be moulded in binder or binder-less sand moulds. In order to increase the firmness of the mould, flasks are vibrated during filling sand.[5] When molten metal front comes in contact with pattern, foam will be degraded, and pyrolysis products of foam degradation will penetrate across the refractory coating and also perimeter sand and finally will come out from the mould. In LFC process, mould filling and its velocity, mould heat transfer, solidification process and casting defects are directly related to the polymer foam degradation, pyrolysis products elimination and the coating characteristics such as thickness.[6]

Department of Metallurgical and Materials Engineering, Iran University of Science and Technology (IUST), 16844 Tehran, Iran

*Corresponding author, email Divandari@iust.ac.ir

Coating is a thin layer of refractory material that controls the pattern firmness, surface smoothness, permeability of polymer foam degradation products and, to some extent, the heat transfer and solidification of casting.[6–14] Increasing the coating thickness decreases fluidity in mould because of the reduction in the permeability and the possibility of prevention of the escape of foam degradation products in cavity; on the other hand, using the thicker refractory coating causes longer fluidity due to the saving of heat contain and decreasing of the cooling rate of the casting.[15]

In the LFC process, mould filling is also dependent on casting geometry. Volume/area (V/A) proportion demonstrates the heat amount, which should be extracted from casting, and P parameter (pattern area) indicates the coating ability for exiting the pyrolysis products. Therefore, with increase in the above mentioned parameters, fluidity of molten metal will increase. A deeper understanding of mould filling characteristics, in foundry industries, is too important in order to minimise the casting defects in thick sections and also to fill the thin wall sections.[16–18]

The driving force of molten metal movement is the potential energy of sprue height and weight, considering that the polymer pattern is a barrier to molten metal front moving.[16–19] Researchers believe that the mould filling behaviour carry out three main mechanisms and is under control of polymer degradation process, back pressure of gaseous products generated as a result of the pyrolysis of foam[20,21] and by wetting and wicking phenomena of liquid pyrolysis products in low melting temperature alloys.[19,22]

Thermal analysis (TA) techniques monitor the temperature changes in a sample as it cools through a phase

© 2010 W. S. Maney & Son Ltd.
Received 12 October 2008; accepted 28 April 2009
DOI 10.1179/174313309X449291

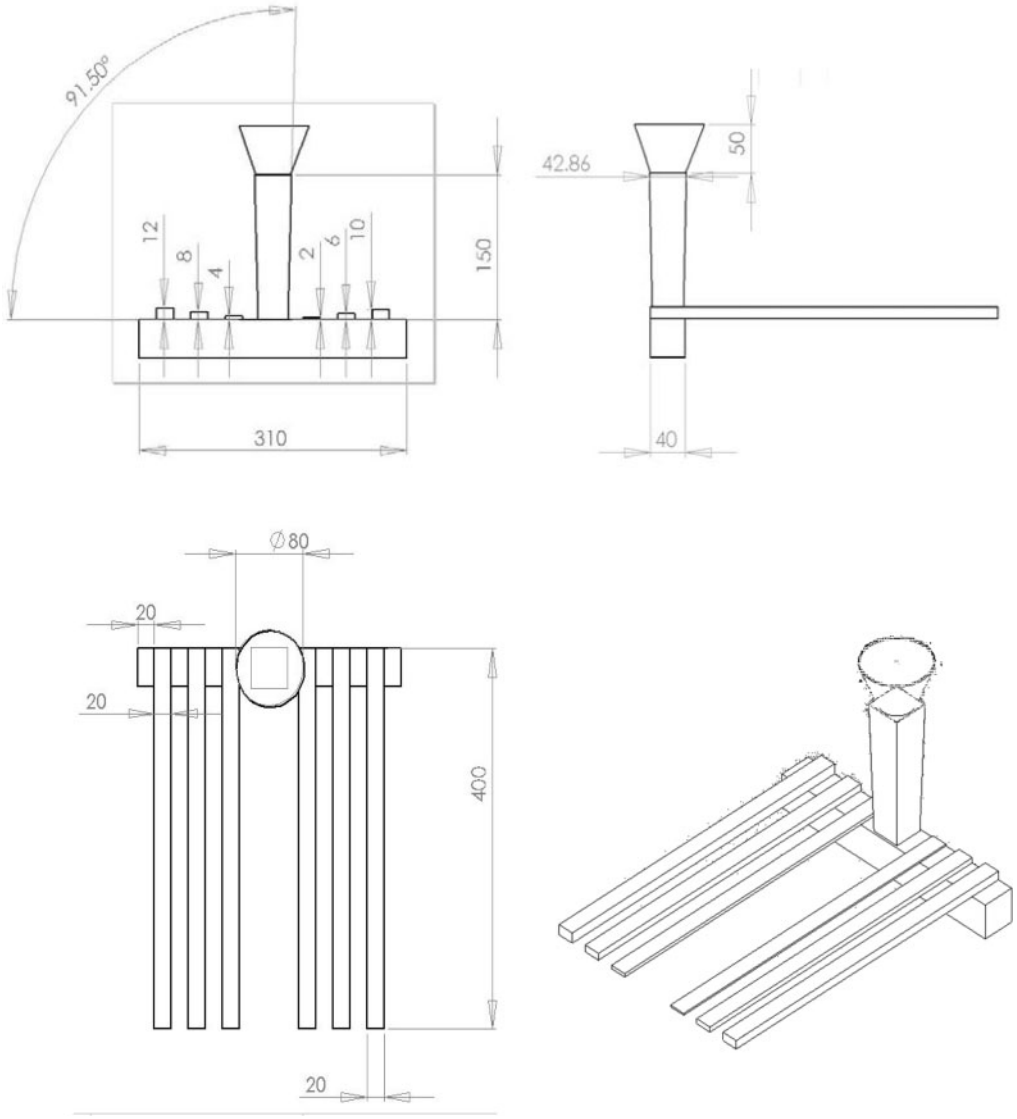

1 Schematic of gating system

transformation interval. The temperature changes in the material are recorded as a function of the heating or cooling time, in such a manner that allows the detection of phase transformations and also cooling rate calculation.[23–26] Thermal analysis of alloys can also provide information about the composition of the alloy, the latent heat of solidification, the evolution of the fraction solid, the types of phases that solidify and even dendrite coherency. There are even more other uses for TA such as determining dendrite arm spacing, degree of modification and grain refining in aluminium alloys, the liquidus and solidus temperatures, characteristic temperatures related to the eutectic regions and intermetallic phase formation.[27–35]

The objectives of the present work were to study the effects of different coating and casting section thicknesses on fluidity of A356 aluminium alloy by means of the Campbell fluidity pattern[36] and also the effect of coating thickness on molten metal velocity by using TA equipment in LFC process.

Experimental procedure

Commercial A356 aluminium alloy ingots were used in this study. The chemical composition is given in Table 1. The alloy was melted in an electric resistance furnace and maintained at a temperature of $790 \pm 5^{\circ}C$. After melting, the oxide layer on the surface was skimmed, and the melt was poured into prepared moulds.

A simple hot wire cutter was used for cutting the strips with thickness of 2, 4, 6, 8, 10 and 12 mm respectively and the dimensional accuracy of $\pm 0{\cdot}2$ mm. Nominal density of polystyrene used in this work was 25 kg m^{-3}. Gating system was designed as depicted in Fig. 1 according to the Campbell fluidity test.[36]

Table 1 Chemical composition of A356 aluminium alloy used

	Elements											
Alloy composition	Al	Si	Mg	Fe	Cu	Mn	Zn	Ti	Cr	Ni	Pb	Sn
A356	Bal.	6·80	0·33	0·35	0·08	0·06	0·04	0·02	<0·01	0·01	0·03	<0·01

Expanded polystyrene patterns were coated by a commercial (Styromol 702) coating made by Foseco (Table 2). In order to study the effect of coating thicknesses on fluidity, six different coating thicknesses were employed on EPS patterns using the dipping method. To achieve various thicknesses, viscosity of slurry was changed by adding water to the water based refractory coating while it was continuously mixing. After dipping, coated patterns were dried in ambient temperature for 24 h. Then, coating thicknesses were measured in 10 points in the length of each test bars by using the (Image Tool for Primavera) software and microscopic images taken from pattern's coating as given in Table 3.

Moulding process was performed in CO_2 bonded silica sand with AFS number 191. To ease the exit of foam pyrolysis products from the mould, after burying the pattern in sand, vent holes were used in every 30 mm over the strips.

In order to measure the velocity of molten metal in different points, TA was performed on all samples using thermocouples K type (Ni–Cr–Ni–0·8 mm diameter), and data were acquired, with $\pm 1^{\circ}C$ resolution and interval times of 0·05 s, by a data acquisition system (A/D converter) linked to a PC. The analogue to digital (A/D) converter used in this work had a sensitive 8 bit converter (a resolution of $1/2^8$ or 0·39%) and a high accuracy of detection. The latest version of the TA program (next view 4-bmcm) was a part of the TA system, which simultaneously displays the cooling curves and temperature and time on the PC monitor for an instant observation.

Four thermocouples were installed in each strip with 30 mm space between them, as shown in Fig. 2. The necessary time data to calculate the velocities were processed using the TA program and Microsoft Excel software. Metallographic samples were sectioned vertically, where the tips of the thermocouples were located, and they were prepared by standard grinding and polishing procedures. The final stage of polishing was done using commercial aluminium oxide paste, and samples were etched by 0·5%HF. Optical microscopy was used to characterise the microstructure.

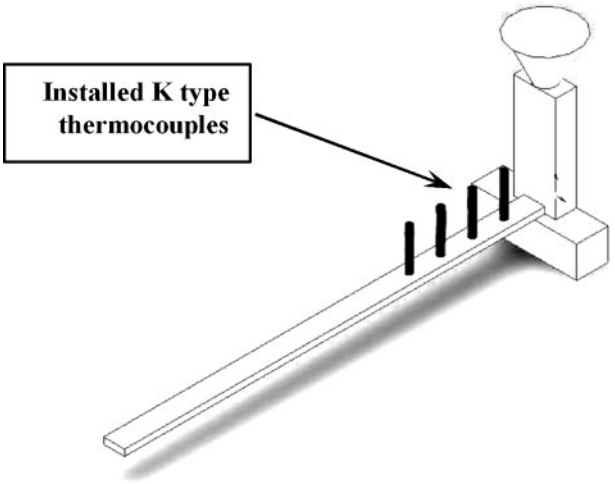

2 Schematic of thermocouples installation

Results and discussion

Effect of strip section thickness on fluidity

Figure 3 shows the effect of the strip thickness on the fluidity of A356 alloy in LFC process. As the strip thickness increases from 2 to 12 mm (and also *V*/*A* proportion increases as Table 4), the fluidity increases from 42 to 225 mm.

In the LFC process, mould filling and fluidity behaviour depends on the *V*/*A* proportion (casting module) and P (section perimeter), while these two parameters are directly related to the casting section thickness.[12] When casting thickness increases, *V*/*A* increases consequently, and because of the extension of solidification time, the fluidity of molten metal will increase. Indeed, *V*/*A* proportion demonstrates the heat content of metal, which will transfer to the sand mould and finally to the surrounding surface during solidification process.

On the other hand, with increasing casting thickness, *P* parameter also increases. When the perimeter of casting increases, the elimination of the polystyrene pyrolysis products (including gaseous and liquidus phases) from the mould cavity to refractory coating pores and later to the sand mould will be easier. This phenomenon happens because the expulsion of the foam degradation products across the molten metal and also the polymer is practically impossible, so pyrolysis products have just one way to go out from the cavity, which is the gaseous gap in front of the moving molten metal.[16,18] Therefore, the larger the section perimeter, the easier the expelling of polystyrene pyrolysis products

Table 3 Coating thicknesses obtained by Image Tool software measurement

Sample no.	Coating thickness, μm	Standard deviation, μm
1	140	8·9
2	170	10·1
3	250	11·7
4	280	7·5
5	350	8·7
6	520	6·9

Table 4 Casting modules of strips with different section thicknesses

Strip thickness, mm	2	4	6	8	10	12
Module (*V*/*A*)	0·9	1·65	2·28	2·82	3·28	3·7

Table 2 Characteristics of used refractory coating

Coating commercial name	Characteristics	Recommended application
Styromol 702	Black coating; water based; containing mixture of graphite and other refractories; Baume number, 65–70	EPS pattern coating in LFC processes

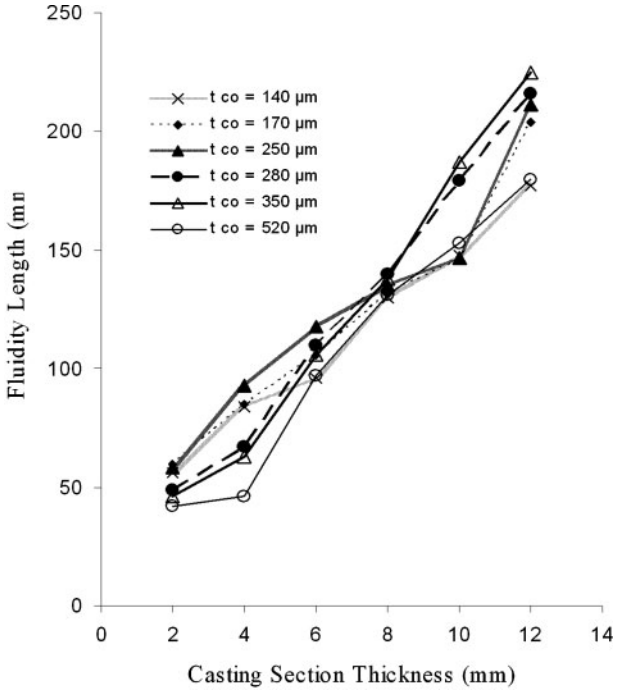

3 Effect of strip casting thickness on fluidity of A356 alloy in LFC process

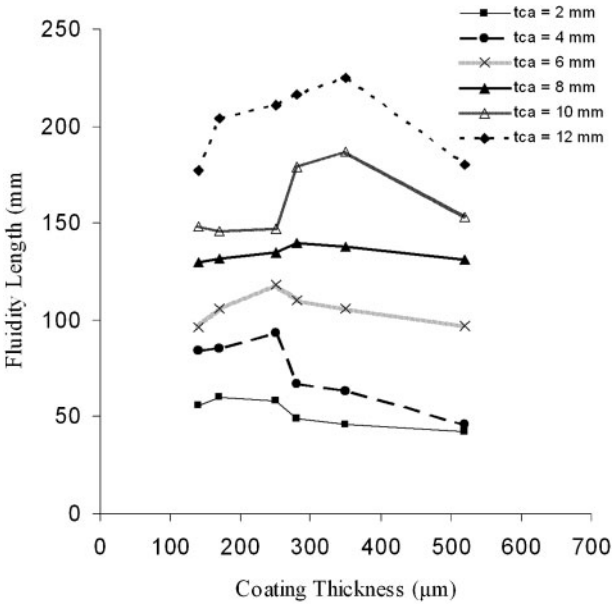

4 Effect of coating thickness on fluidity of A356 alloy in LFC process

to coating pores and sand mould and, consequently, the longer the fluidity length of molten metal.

The linear equations of the fluidity length of A356 alloy as a function of strip thickness and various coating thicknesses (140, 170, 250, 280, 350 and 520 μm respectively) were obtained.

$$L_f\,140 = 11{\cdot}871 t_{ca} + 32{\cdot}067 \quad (1)$$

$$L_f\,170 = 13{\cdot}4141 t_{ca} + 27{\cdot}933 \quad (2)$$

$$L_f\,250 = 13{\cdot}343 t_{ca} + 33{\cdot}933 \quad (3)$$

$$L_f\,280 = 17{\cdot}129 t_{ca} + 6{\cdot}6 \quad (4)$$

$$L_f\,350 = 18{\cdot}586 t_{ca} + 2{\cdot}2667 \quad (5)$$

$$L_f\,520 = 14{\cdot}929 t_{ca} + 3{\cdot}6667 \quad (6)$$

The coefficient of correlation for mentioned equations are 0·9952, 0·9788, 0·9704, 0·9961, 0·9935 and 0·9856 respectively, and the average slope of the equations that indicates the effect of casting thickness on the fluidity is 14·879.

Ajdar *et al.*[37] showed the effect of casting thickness on the fluidity length as below.

$$L_f = \frac{\rho_L v a}{2h_g(T_m - T_i)}\left(C_L \Delta T + \frac{H_L}{2} - \frac{H_E \rho_P}{\rho_L}\right) \quad (7)$$

where L_f is the fluidity length (mm), ρ_L is the molten metal density (g mm^{-3}), V is the molten metal velocity (mm s^{-1}), a is the casting section thickness (mm), h_g is the heat transfer coefficient (w mm^{-2}/°), T_m is the metal melting temperature (°C), T is the ambient temperature (°C), C_L is the molten metal heat capacity (°C J g^{-1}), ΔT is the super heat (°C), H_L is the latent heat (J g^{-1}), H_E is the chemical degradation energy of foam pattern (J g^{-1}), and ρ_P is the density of foam pattern (g mm^{-3}).

As the equation (7), the fluidity length L_f has direct proportion to casting section casting.

Effect of coating thickness on fluidity

Figure 4 shows the effect of coating thickness on the fluidity length of A356 aluminium alloy in LFC. As seen in this figure, increasing the thickness of coating on each strips caused a specific maximum fluidity length for each casting section thickness. As the strip thickness increases, from 2 to 12 mm, the maximum fluidity lengths were obtained in a thicker refractory coating thicknesses. For example, optimum coating thicknesses to reach maximum fluidity length for 2, 4, 6, 8, 10 and 12 mm strips are 170, 250, 250, 280, 350 and 350 μm respectively.

Reciprocity of two different characteristics of LFC refractory coatings, including heat and mass transfer, is the reason of these dissimilar results. On the one hand, coating is used in evaporative pattern casting as heat insulator to save the heat content of molten metal and increase the fillability of metal to obtain perfect thin wall sections in complicated patterns; on the other hand, the coating can acts as a preventive parameter for the expelling of gaseous products from the mould.

In LFC, the interface consists of three components: the interface between the casting and the coating; the coating itself and the interface between the coating and mould, as depicted in Fig. 5. Also shown in Fig. 5*a* is the temperature profile across the interface. The two temperature discontinuities, one between the casting and the coating and the other between the coating and the mould surface, represent the interfacial thermal resistances at these locations. These thermal resistances arise from imperfect contact between the moulding materials.

Thus, generally in LFC, the overall interfacial heat transfer is a function of L_r (refractory coating thickness), h_{cr} (heat transfer coefficient between casting and refractory coating), h_{rm} (heat transfer coefficient between refractory coating and mould) and k_r (refractory coating thermal conductivity). Since the reciprocal of h denotes thermal resistance, the interfacial heat

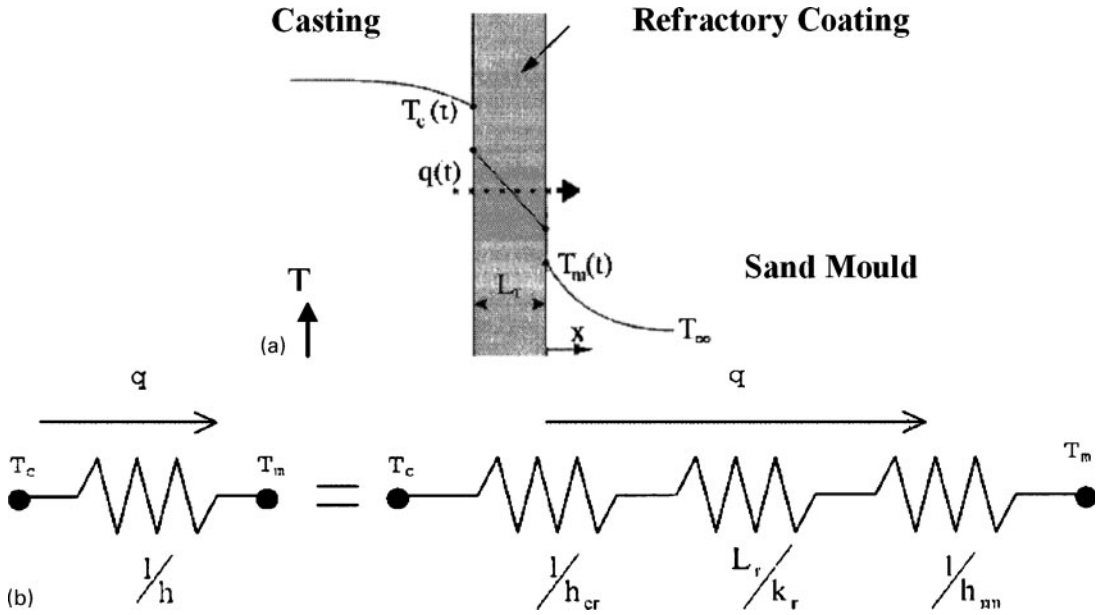

5 ***a*** **sketch of interface with temperature profile across it and** ***b*** **resistor diagram of thermal resistance across interface**

transfer can be described using a 'resistor diagram', per unit area, as is depicted in Fig. 5*b*. Therefore, the overall interfacial heat transfer coefficient h is related to the total thermal resistance by

$$h = \frac{1}{\Sigma R} = \frac{1}{1/h_{\mathrm{er}} + L_2 + 1/h_{\mathrm{rm}}} \tag{8}$$

According to equation 8, in the LFC process, as the coating thickness increases, thermal resistance increases. Thermal resistance represents the difficulty of heat extraction from the casting during solidification, which means that at a low thermal resistance, the rate of heat transferring of casting is high. In other words, refractory coatings in the LFC should be able to permit the crossing of the polymer degradation products thoroughly in order to prevent defect in casting and also increase fluidity of molten metal, which may not be fulfilled if the permeability of the coating is not enough. Therefore, in a certain casting condition, in the LFC processes, coating with a specific thickness should be used to balance the mentioned characteristics of coatings in order to reach the optimum fluidity length.

In the present work, appropriate coating thickness for thinner casting sections was thinner in comparison with proper coating thickness for thicker sections, e.g. for 2 mm strip, the best coating thickness was 170 μm, and for 12 mm casting section, it was 350 μm. It means that permeability characteristic of the coating is more important in thin casting sections, and one has to adjust the coating in such a manner that the permeability overcomes the heat insulating characteristic in this condition.

The polymer degradation products, in thin casting sections, have possibly the main role in the fluidity of molten metal; therefore, if the thickness of coating increases, consequently, the permeability and expulsion of the products will decrease, and fluidity will be affected by imprisoned products of the degraded foam, such as demonstrated in Fig. 6. This figure shows an image taken from the edge of the sample with 520 μm coating thickness. Porosity, which is possibly created by pyrolysis products, can be seen in this figure, emphasising the importance of measuring optimum thickness for casting.

Effect of coating thickness on molten metal velocity

To study the effect of coating thickness on the velocity of molten metal, four thermocouples were installed in a single 12 mm strip as shown in Fig. 2. The distance of the first thermocouple to the runner was 30 mm, and the distance between each of them was also 30 mm. For every 30 mm length of each strip, with specific coating thickness, the velocity was measured, as shown in Fig. 7.

The velocity of the molten metal in the first 30 mm length, near the runner, is independent on the coating thickness, as indicated in Fig. 7. It means that, at the beginning of the strip, the amounts of gaseous and liquid products resulting from the foam degradation are too low to prevent the fluid flow, consequently decreasing the velocity of molten metal. On the other hand, the heat content of molten metal is high enough to provide the movement energy of the fluid in this region.

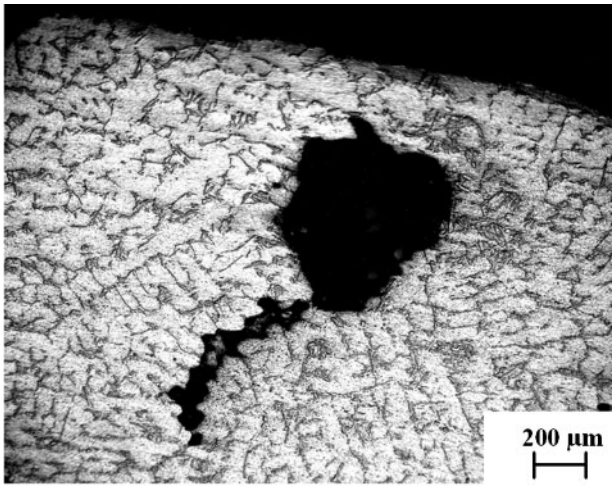

6 Microstructure of casting showing blow defects in strip with 520 μm coating thickness

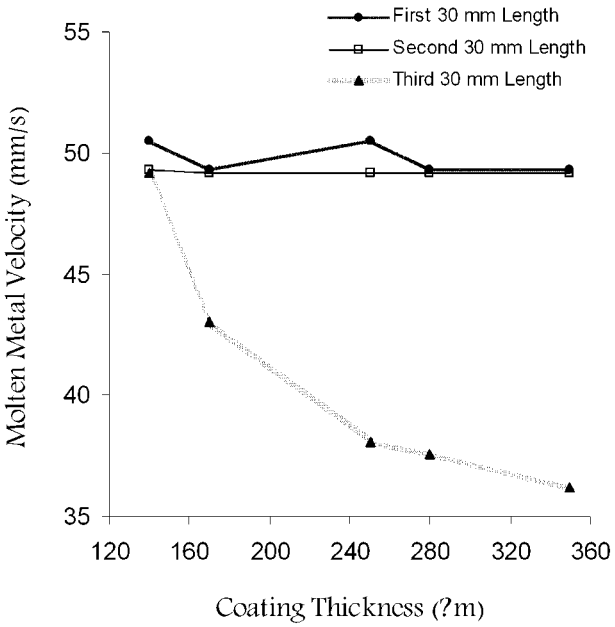

7 Effect of coating thickness on velocity of molten metal in first, second and third 30 mm length of strip

In the second 30 mm length of the runner, the mass and heat transfer characteristics of the refractory coating have been balanced, and as a result, the molten metal velocity of all samples with different coating thicknesses was almost similar. It means that, in this region, the fluid velocity is independent on the coating thickness, as also indicated in Fig. 7. In this region, neither heat transferring characteristic of coating nor mass transferring and expelling characteristic have overcome each other, and therefore, the velocity remained constant.

Molten metal velocity, in the third 30 mm space of the runner, decreased as the coating thickness increased. It means that the amount of polymer pyrolysis products and its accumulation, possibly because of the problem of expulsion, have increased to an extent that it has affected the molten metal movement, as has been reported by other's work.[18] This means that, in this region, mass transferring characteristic has overcome the heat insulating characteristic of the coating.

Microstructure

The microstructures of some samples are shown in Fig. 8. These figures belonged to strips with 2, 6 and 12 mm section thicknesses respectively. They were selected from the strips coated with the coating thickness in the range of 280 ± 25 μm. Samples with thinner casting sections, solidified at a higher cooling rate, showed a finer DAS, as can be seen in these figures. Naturally, increasing the casting section thickness will cause coarsening of the dendrite arm spacing, which has been reported by many other researchers.[14,23,24–33,37]

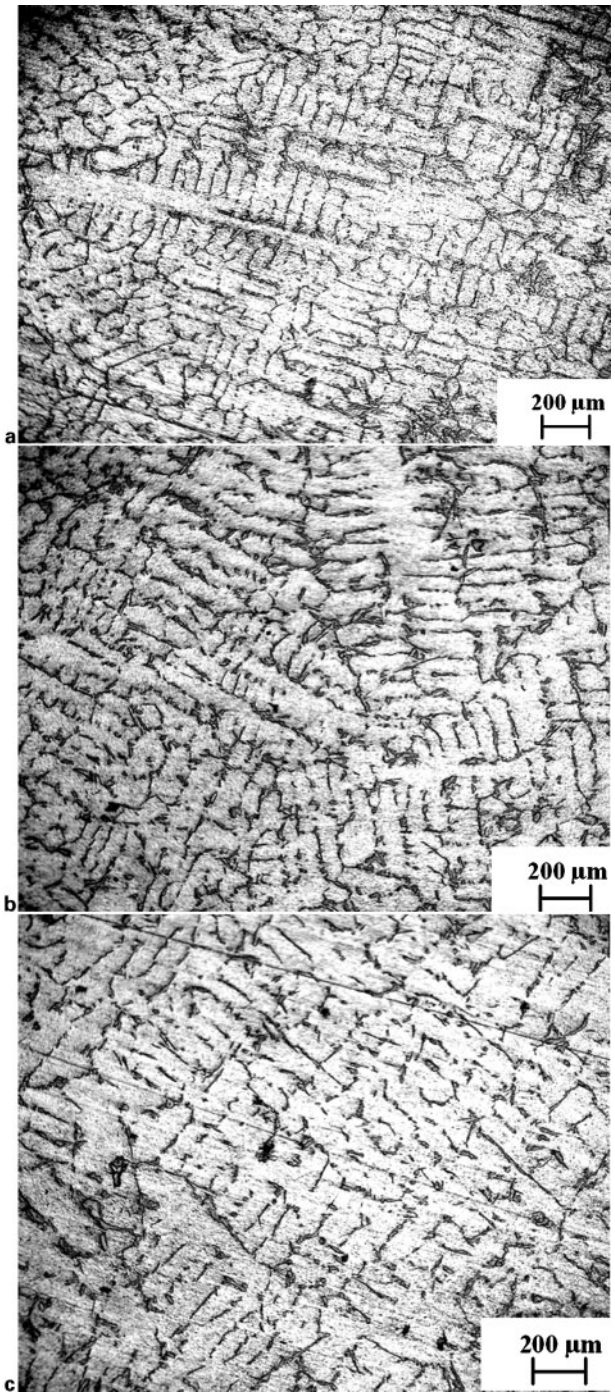

8 Dendritic structure of A356 alloy in *a* 2 mm thick strip having 280 μm coating thickness (35·61 μm DAS), *b* 6 mm thick strip having 280 μm coating thickness (39·91 μm DAS) and *c* 12 mm thick strip having 280 μm coating thickness (49·56 μm DAS)

Conclusion

The effect of refractory coating thickness and casting section thickness on the fluidity and also the effect of coating thickness on the molten metal velocity in the strips produced via LFC process were studied. The results are summarised as follows.

1. A direct relation was found between fluidity length and the casting section thickness. As the casting thickness increased from 2 to 12 mm, fluidity length increased from 42 to 225 mm for different coating thicknesses.

2. Fluidity length was noticed to be under effect of refractory coating thickness. As the casting section thickness increased, the maximum fluidity lengths were obtained at thicker refractory coating thicknesses, using various coating thickness in each experiments. Optimum coating thicknesses, in order to reach maximum fluidity length, for strips with 2, 4, 6, 8, 10 and 12 mm section

thickness were 170, 250, 250, 280, 350 and 350 μm respectively.

3. The velocity of molten metal was affected by coating thickness in specific distances from runner. In the first 30 mm near the runner, velocity was independent of the thickness of coating because of the reciprocity of mass and heat transfer characteristic of refractory coating. In the second 30 mm length, the metal velocities were almost the same in all the specimens, and in the third 30 mm length, the molten metal velocity was decreased due to strong effect of the back pressure on metal front.

References

1. 'Metals handbook', Vol. 15, 9th edn, 230–234; 1985, Metals Park, OH, ASM.
2. S. Saghi, M. Divandari and Y. H. K Kharrazi: *Iran. J. Mater. Sci. Eng.*, 2004, **1**, (2), 31–38.
3. Y. H. K Kharrazi, M. Divandari and S. Saghi: *Iran. J. Mater. Sci. Eng.*, 2005, **2**, (1), 25–32.
4. H. E. Littleton, B. A. Miller, D. Sheldon and C. E. Bates: *AFS Trans.*, 1996, **104**, 335–346.
5. D. S. Sheldon: *AFS Trans.*, 2002, **110**, 1–14.
6. O. Gurdogan: *AFS Trans.*, 1996, **104**, 451–459.
7. S. Shivkumar, X. Yao and M. Makhlouf: *Scr. Metall. Mater.*, 1995, **33**, (1), 3946.
8. P. Kannan, J. J. Biernacki and D. P. Visco, Jr: *J. Anal. Appl. Pyrolysis*, 2007, **78**, 162–171.
9. X. J. Liu, S. H. Bhavnani and R. A. Overfelt: *J. Mater. Process. Technol.*, 2007, **182**, 333–342.
10. S. M. H. Mirbagheri, H. Esmaeileian, S. Serajzadeh, N. Varahram and P. Davami: *J. Mater. Process. Technol.*, 2003, **142**, 493–507.
11. S. Ji, M. Sirvio, J. J. Vuorinen and J. Ordas: *AFS Trans.*, 1999, **107**, 779–786.
12. J. Fu, H. L. Tsai and D. R. Askeland: *AFS Trans.*, 1995, **103**, 817–828.
13. S. Mehta and S. Shivkumar: *AFS Trans.*, 1995, **103**, 663–668.
14. X. Yao and S. Shivkumar: *AFS Trans.*, 1995, **103**, 761–765.
15. M. D. Lawrence, C. W. Ramsay and C. R. Askeland: *AFS Trans.*, 1998, **106**, 349–356.
16. M. Khodai and N. Parvin: *J. Mater. Process. Technol.*, 2008, **206**, 1–6.
17. Z. Liu, J. Hu, Q. Wang, W. Ding, Y. Zhu, Y. Lu and W. Chen: *J. Mater. Process. Technol.*, 2002, **120**, 94–100.
18. Y. Sun, H. L. Tsai and D. R. Askeland: *AFS Trans.*, 1995, **103**, 651–662.
19. X. Liu, C. W. Ramsay and D. R. Askeland: *AFS Trans.*, 1994, **102**, 903–914.
20. C. M. Wang, A. J. Paul, W. W. Finchero and O. Huey: *AFS Trans.*, 1993, **101**, 897–904.
21. H. L. Tsai and T. S. Chen: *AFS Trans.*, 1998, **106**, 881–890.
22. Y. Sun, H. L. Tsai and D. R. Askeland: *AFS Trans.*, 1992, **100**, 297–308.
23. W. Kurz and D. J. Fisher: 'Fundamentals of solidification'; 1998, Rockport, Trans. Tech. Publication.
24. L. Backuerud, G. Chai and J. Tamminen: 'Solidification characteristics of aluminum alloys', Vol. 2, 'Foundry alloys'; 1990, Stockholm, AFS/Skanaluminium.
25. J. Tamminen: 'Thermal analysis for investigation of solidification mechanisms in metals and alloys', PhD thesis, University of Stockholm, Sweden, 1998.
26. T. Hatakeyama and L. Zhenhai: 'Handbook of thermal analysis', 3–6; 1998, Chichester, New York, John Wiley and Sons.
27. S. G. Shabestari and M. Malekan: *J. Can. Metall. Q.*, 2005, **44**, (3), 305–312.
28. S. Gowri: *AFS Trans.*, 1994, **102**, 503–508.
29. L. Ananthanarayanan, F. H. Samuel and J. Gruzleski: *AFS Trans.*, 1992, **100**, 383–391.
30. A. M. Samuel, P. Ouellet, F. H. Samuel and H. W. Doty: *AFS Trans.*, 1997, **105**, 951–962.
31. J. O. Barlow and D. M. Stefanescu: *AFS Trans.*, 1997, **105**, 349–354.
32. R. I. MacKay, M. B. Djurdjevic, H. Jiang, J. H. Sokolowski and W. J. Evans: *AFS Trans.*, 2000, **108**, 511–520.
33. D. Emadi and L. V. Whiting: *AFS Trans.*, 2002, **110**, 200–209.
34. M. B. Djurdjevic, W. T. Kierkus, G. E. Byczynski, T. J. Stockwell and J. H. Sokolowski: *AFS Trans.*, 1999, **107**, 173–179.
35. M. B. Djurdjevic, W. T. Kierkus, R. E. Liliac and J. H. Sokolowski: 'Extended analysis of cooling curves', Proc. 41th Conf. of Metal, Montreal, Canada, 2002, CIM, 351–365.
36. M. Emamay and J. Campbell: *Cast Met.*, 1995, **8**, 13–20.
37. R. Ajdar, C. Ravindran and A. Melean: *AFS Trans.*, 2002, **110**, 122–147.